

## Probing a quantum Hall pseudospin ferromagnet by resistively detected nuclear magnetic resonance

G. P. Guo,<sup>1</sup> X. J. Hao,<sup>1</sup> T. Tu,<sup>1,\*</sup> Y. J. Zhao,<sup>1</sup> Z. R. Lin,<sup>1</sup> G. Cao,<sup>1</sup> H. O. Li,<sup>1</sup> C. Zhou,<sup>1</sup> G. C. Guo,<sup>1</sup> and H. W. Jiang<sup>2,†</sup>

<sup>1</sup>Key Laboratory of Quantum Information, Chinese Academy of Sciences, University of Science and Technology of China, Hefei 230026, People's Republic of China

<sup>2</sup>Department of Physics and Astronomy, University of California at Los Angeles, 405 Hilgard Avenue, Los Angeles, California 90095, USA

(Received 17 December 2009; published 14 January 2010)

Resistively detected nuclear magnetic resonance (RD-NMR) has been used to investigate a two-subband electron system in a regime where quantum Hall pseudospin ferromagnet (QHFP) states are prominently developed. It reveals that the easy-axis QHFP state around the total filling factor  $\nu=4$  can be detected by the RD-NMR measurement. Approaching one of the Landau-level (LL) crossing points, the RD-NMR signal strength and the nuclear-spin-relaxation rate  $1/T_1$  enhance significantly, a signature of low-energy spin excitations. Furthermore, the RD-NMR signal at another identical LL crossing point is surprisingly missing which presents a puzzle. These observations demonstrate that the spin freedom may play an role in the understanding of the QHFP states.

DOI: [10.1103/PhysRevB.81.041306](https://doi.org/10.1103/PhysRevB.81.041306)

PACS number(s): 73.43.Nq, 71.30.+h, 72.20.My

The multicomponent electron systems have been continuously drawing intensive research interest because of its ground states and excitations.<sup>1</sup> In experimental systems, different Landau levels (LLs) can be tuned to cross by varying gate voltage, charge density, magnetic field, or the magnetic field tilted angle to the sample. Electron-electron correlations become particularly prominent when two or more sets of LLs with different layer, subband, valley, spin, or orbital indices are brought into degeneracy.<sup>1-8</sup> Recent experiments in single quantum well with two subbands occupied systems,<sup>5,6</sup> providing a useful laboratory for addressing these issues, showed evidence of the formation of quantum Hall pseudospin ferromagnets (QHFPs) due to the interactions of the two subbands (termed as pseudospins) around the LLs crossing point. The QHFPs taking place at total filling factor  $\nu=3, 5$  and  $\nu=4$  are easy-plane or easy-axis QHFPs, respectively, depending on the details of the two subbands configurations. In spite of many recent theoretical advances,<sup>9-12</sup> a comprehensive understanding is not yet achieved. Thus far, experimental and theoretical studies all focused on the pseudospin freedom. However, in this work we would address the unique spin excitations in the QHFP states.

To address the question what spin states are in two-subband systems in nature, measurements other than the conventional transport and optical means are needed. Since the Zeeman energy of nuclear spin is about three orders of magnitude smaller than that of electron spin, exchange of spin angular momentum between the electron and nuclear spin is allowed only when the electron system supports spin excitations with low energy. The nuclear-spin-relaxation rate  $1/T_1$  thus probes the density of states at low energy of the electron-spin system that cannot be accessed by other means. The resistively detected NMR (RD-NMR) technique has recently emerged as an effective method to probe collective spin states in the fractional quantum Hall regime,<sup>13,14</sup> the Skyrmion spin texture close to the filling factor 1,<sup>14-16</sup> the role of electron-spin polarization in a bilayer system,<sup>17-19</sup> and the ferromagnetic state accompanied by collective spin excitations of a two-subband system.<sup>20</sup> Here we use this

technique to study spin freedom and its relation with pseudospin in the vicinity of the QHFP states at filling factor  $\nu=3, 4, 5$ . It reveals that the easy-axis QHFP state at  $\nu=4$  is sensitive to the RD-NMR measurement. As approaching to one LL crossing point at  $\nu=4$  where the easy-axis QHFP phase is well developed, the RD-NMR signal strength and the nuclear-spin-relaxation rate  $1/T_1$  enhance quickly which may be due to the low-energy spin excitations there. Furthermore, the RD-NMR signal can be suppressed anomaly at another identical LL crossing point of  $\nu=4$ .

The sample was grown by molecular-beam epitaxy and consists of a symmetrical modulation-doped 24-nm-wide single GaAs quantum well bounded on each side by Si  $\delta$ -doped layers of AlGaAs with doping level  $n_d=10^{12}$  cm<sup>-2</sup>. Heavy doping creates a very dense 2DEG, resulting in the filling of two subbands in the well. As determined from the Hall resistance data and Shubnikov-de Haas oscillations in the longitudinal resistance, the total density is  $n=8.0 \times 10^{11}$  cm<sup>-2</sup>, where the first and the second subband have a density of  $n_1=6.1 \times 10^{11}$  cm<sup>-2</sup> and  $n_2=1.9 \times 10^{11}$  cm<sup>-2</sup>. The sample has a low-temperature mobility  $\mu=4.1 \times 10^5$  cm<sup>2</sup>/V s, which is extremely high for a 2DEG with two filled subbands. A 100  $\mu$ m wide Hall bar with 270  $\mu$ m between voltage probes was patterned by standard lithography techniques. A NiCr top gate was evaporated on the top of the sample, approximately 350 nm away from the center of the quantum well. By applying a negative gate voltage on the NiCr top gate, the electron density can be varied continuously. Several turns of NMR coil were wound around the sample, which was placed in a top-loading dilution refrigerator with a base temperature of 15 mK. A small radio frequency (rf) magnetic field generated by the coil with a matching frequency  $f=\gamma H_0$  will cause NMR for <sup>75</sup>As nuclei, where the gyromagnetic ratio  $\gamma=7.29$  MHz/T. The resistance was measured using quasi-dc lock-in technique with 11.3 Hz.

In the present work, we refer the first and second subbands to as symmetric and antisymmetric states. In the pseudospin language, one of them can be labeled as pseudospin

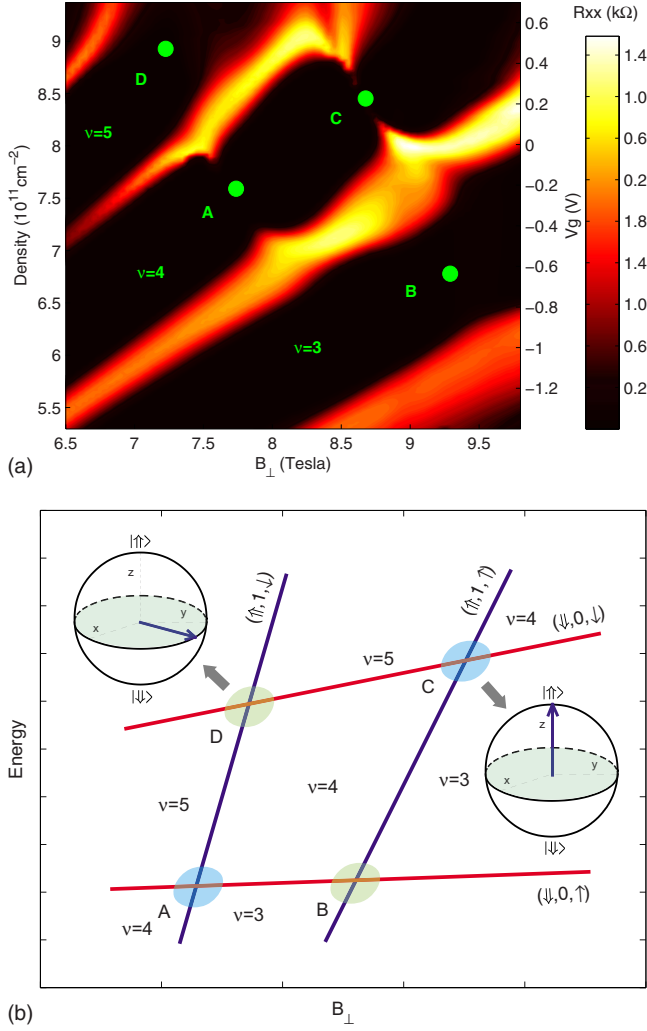


FIG. 1. (Color online) (a) The longitudinal resistance  $R_{xx}$  in the density ( $n$ )—magnetic field ( $B_{\perp}$ ) phase diagram at filling factor  $\nu=3, 4, 5$ , which are measured at the base temperature. (b) Schematic drawing of the crossing between different indices Landau levels and resulting easy-plane or easy-axis pseudospin states at points B, D and A, C, as correspondingly marked in Fig. 1(a).

up ( $\uparrow$ ) and the other as pseudospin down ( $\downarrow$ ). When a magnetic field  $B_{\perp}$  is applied, the energy spectrum of the quantum well discretizes into a sequence of Landau levels. We label the single-particle levels  $(i, N, \sigma)$ , which  $i$  ( $=\uparrow, \downarrow$ ),  $N$ , and  $\sigma$  ( $=\uparrow, \downarrow$ ) are the pseudospin, orbital, and spin quantum numbers. In the present work we have concentrated our study around the filling factor  $\nu=3, 4, 5$ , where the filling factor  $\nu$  denotes the number of filled Landau levels. The longitudinal resistance  $R_{xx}$  in the density ( $n$ )—perpendicular magnetic field ( $B_{\perp}$ ) plane exhibits a squarelike structure around  $\nu=3, 4, 5$ , as shown in Fig. 1(a). The most noticeable feature of the squarelike structure is the disappearance of the extended states (i.e., bright lines) on its four boundaries, marked by A, B, C, D in Fig. 1(a). Here point A corresponds to the degeneracy point of  $|\uparrow, 1, \downarrow\rangle$  and  $|\downarrow, 0, \uparrow\rangle$ , point B corresponds to that of  $|\uparrow, 1, \uparrow\rangle$  and  $|\downarrow, 0, \uparrow\rangle$ , point C corresponds to that of  $|\uparrow, 1, \uparrow\rangle$  and  $|\downarrow, 0, \downarrow\rangle$ , point D corresponds to that of  $|\uparrow, 1, \downarrow\rangle$  and  $|\downarrow, 0, \downarrow\rangle$ , as illustrated sche-

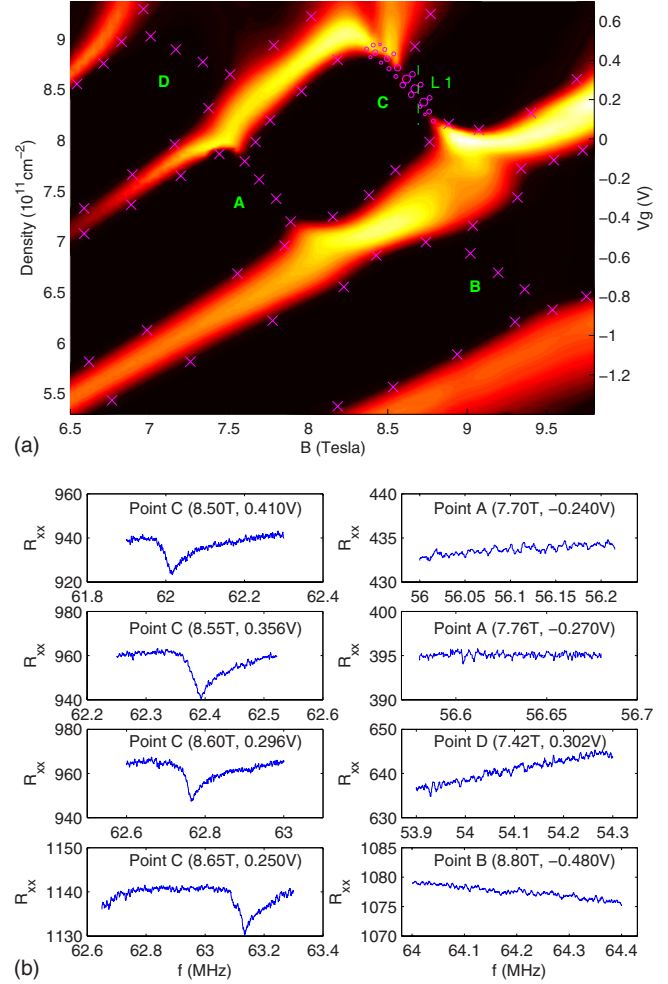


FIG. 2. (Color online) (a) The NMR signals phase diagram of the sample at  $\nu=3, 4, 5$ . The cross and circle symbols in the map denote the places where the NMR signals are measured. The “ $\times$ ” mean places where there are no NMR signals, while the “ $\circ$ ” show the places where the NMR signals are observed. And the size of “ $\circ$ ” symbols give a schematic illustration of the strength of NMR signals. The dashed line L1 is the trace along which we measured NMR signal as shown in Fig. 5. (b) Typical resistively detected NMR spectrum measured around point C and A, B, D.

matically in the Landau-level fan diagram Fig. 1(b). The disappearance and result square structure represents a pseudospin ferromagnet, which is due to the opening pseudo-spin gaps of easy-plane or easy-axis pseudospin ferromagnetic states, respectively, at the level crossing points of B, D and A, C, as depicted in Fig. 1(b).<sup>4-6,9</sup>

RD-NMR, performed in the proximity of the square structure, reveals prominent (absent) NMR signal at different regions. In order to get a clear signal and minimize heat effect, most of experiments were carried out with a rf power of 0 dBm and the power of the rf at the sample is estimated to below 0.1 mW. As shown in Fig. 2(a), the cross and circle symbols in the map denote the places where the NMR signals are measured. The cross “ $\times$ ” means the places where there are no NMR signals, while the circle “ $\circ$ ” shows the places where the NMR signals are observed. And the size of “ $\circ$ ” symbols give a schematic illustration of the strength of

NMR signals. From this map we found that the NMR signals only occur at the upper arm of the square structure around crossing point C, while we did not find any signal at the lower arm of this square structure around another crossing point A and its two sides around crossing point B and D.

Now we focused on the region around the LL crossing point C, where pronounced NMR signals were observed. Typical NMR lines around point C are shown in Fig. 2(b). The relative change in  $R_{xx}$  is typically about 1% at resonance. Upon resonance,  $R_{xx}$  in all NMR lines shows a sharp decrease followed by a much slower relaxation process back to its original value, which is characterized by the nuclear-spin-relaxation time owing to the interaction with the electron-spin system,  $T_1$ , as will be discussed below.

We believe the RD-NMR described here is due to the electron and nuclear-spin flip-flop effect.<sup>14,15,20</sup> For the two-dimensional electron system in GaAs, the contact hyperfine interaction with the polarized nuclei acts as an effective magnetic field  $B_N$  for the electron spin. The effective electron spin-flip energy is then reduced,  $E_z = g^* \mu_B B S_z + A \langle I_z \rangle S_z = g^* \mu_B (B + B_N) S_z$  as  $g^* < 0$ . When the NMR resonance condition is matched, the nuclear spins are depolarized and the electron Zeeman energy increases consequently. Since  $R_{xx}$  is dependent on the thermally activated energy gap  $E_a$ ,  $R_{xx} \propto \exp(-E_a/2k_B T)$ , the NMR is manifested by a drop in  $R_{xx}$ , as shown by all the NMR lines in Fig. 2(b). This allows the nuclear-spin polarization to be sensitively detected by a change in the transport coefficient of the electron system  $R_{xx}$ .

The above observations reveals the spin excitation in the square structure is of intrinsic interest and is well correlated with the spin polarization of the easy-axis QHPF states. At point C, when the two competing pseudospin (up and down) states acquire the same energy and leads to easy-axis anisotropy, they separate into domains with opposite pseudospin states.<sup>4,6,9,12,21</sup> On the other hand, the pseudospin up and down states have opposite spins. As a result, magnetic domains form and the electronic state within each domain is described as an Ising-like QH ferromagnet with either one of two possible spin orientations. As the applied current forces electrons to scatter between adjacent domains with different spin but almost degenerate energy, the nuclei in the neighborhood can become polarized and probed by the RD-NMR measurement. However at other crossing point B and D, the QHPF states are easy plane, which means that the two degenerate Landau levels are mixing and no spin magnetization formation. Since easy-plane QHPF state cannot spontaneously separate into magnetic domains, there is no nuclear polarization and the NMR signals are destroyed.

To support the mechanism of the polarized nuclear spins, current dependence of the NMR signal was studied. In this measurement, the sample resistance was measured with a low ac current of 20 nA, while ramping the dc current in a wide range to bias the sample. The result indicates that the NMR signal is enhanced by a factor of five in the low current range to 250 nA and then saturates. The data thus consist with the picture of current induced dynamic polarization.<sup>14,15</sup>

To gain more support of our observation of the nature of the spin in the easy-axis QHPF states, we studied the coupling between the nuclei and the electrons by measuring the

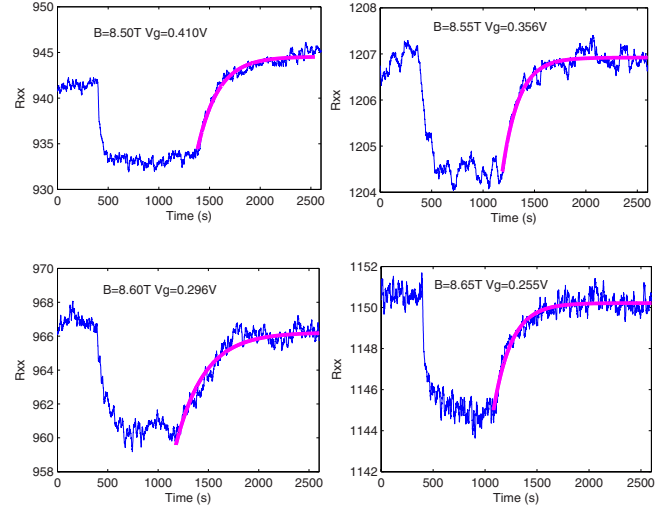


FIG. 3. (Color online) Measuring nuclear-spin-relaxation time  $T_1$  around point C by recording time evolution of  $R_{xx}$  irradiated by rf, initially off resonance, on resonance and finally off resonance.  $T_1$  is determined by an exponential fit to the experiment data.

nuclear-spin-relaxation time  $T_1$ , at various positions near the crossing point C. First, rf was tuned into resonance, and  $R_{xx}$  shows a sharp decrease due to the nuclear depolarization. Then, the frequency was switched back to off resonance. Nuclear spins that have once flopped hardly relax back because of their longer relaxation time  $T_1$ , which is on the order of minutes, relative to that of the electrons. Hence,  $R_{xx}$  slowly relaxes back to its original value, and  $T_1$  can be derived by fitting  $R_{xx}$  to the relation  $R_{xx} = \alpha + \beta \exp(-t/T_1)$ .<sup>14,16</sup> Figure 3 shows the data around point C to determine  $T_1$ .

Further insight is gained by investigating the NMR signals along the line L1 [please see Fig. 2(a)]. As depicted in Fig. 4(a), our measurement shows a clear peak of NMR ratio  $\Delta R_{xx}/R_{xx}$  at the crossing point C where the easy-axis QHPF states is well developed. The obtained values of nuclear-spin-relaxation rate  $1/T_1$  along line L1 are also plotted in Fig. 4(a).  $1/T_1$  rapidly increases from nearly zero to  $8 \times 10^{-3}$  (1/s) toward to the crossing point C, as electron becomes the pseudospin ferromagnetic states. For comparison, in Fig. 4(b) we also show the electron activation energy gap  $E_a$  along the line L1. The single particle energy difference  $E_z$  acts as effective Zeeman energy, and  $E_a$  shows a slope of five

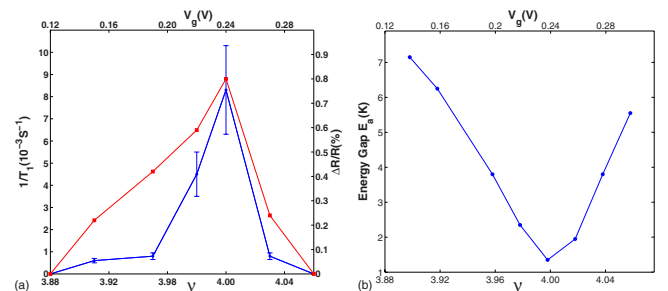


FIG. 4. (Color online) Plot of the RD-NMR signal ratio  $\Delta R_{xx}/R_{xx}$  (red square), nuclear-spin-relaxation rate  $1/T_1$  (blue circle) (a) and electron activation energy gap  $E_a$  (b) against filling factor  $\nu$  along the line L1 [in Fig. 2(a)].

times greater than the single-particle Zeeman gap  $E_z$ . This unusual behavior is likely to be caused by the easy-axis QHPF states.<sup>4,6</sup> We emphasize that along other lines in the phase diagram [Fig. 2(a)], the NMR signal and  $1/T_1$  also show an obvious enhancement as approaching to the crossing point C and demonstrate that  $1/T_1$  is a sensitive indicator of the pseudospin ferromagnet formation. The similarity between these phenomenon strongly suggest that an intimate link between the spin and pseudospin in the easy-axis pseudospin ferromagnetic states.

Interestingly, the data shown in Fig. 4(b) shows that the slope of activation energy gap  $E_a$  to single-particle Zeeman gap is as large as 5, which implies many spin flips within the magnetic domain walls and support low-energy mode of spin excitations.<sup>21-23</sup> Recently, a systematically theoretical calculation<sup>12</sup> using real experimental parameters finds that there is a high spin polarization ( $\sim 50\%$ ) and associated spin fluctuations around the crossing points, which is consistent with our observations. As approaching to the crossing point C, these low-energy spin excitations will give new channels to relax the nuclear spin through the electron and nuclear-spin flip-flop process. Thus the NMR signal ratio  $\Delta R_{xx}/R_{xx}$  and the nuclear-spin-relaxation rate  $1/T_1$  are enhanced.

Despite the fact that the bulk of the results can be understood within the framework of pseudospin quantum Hall ferromagnetism, there is still an apparent puzzle. While we can find very strong NMR signals at the upper arm of the square structure around point C, there is no detectable signal at the lower arm of this square structure around point A even large dc current pulse up to 250 nA or large rf power is applied to enhance possible NMR signals. Since the two points have

equivalent LLs crossing configurations, one would expect that they are the same easy-axis QHPF states and should produce similar NMR responses. In principle, the NMR signal can be suppressed by spin-orbital coupling<sup>24</sup> or mobility of domains.<sup>25</sup> However, in our case, point A and C have identical strength in spin-orbital coupling and disorder. Therefore, the anomalous suppression of NMR signal at point A may suggest that there could be some additional physics which has not yet been recognized in the theory of pseudospin quantum Hall ferromagnetism.

In summary, RD-NMR has been measured in a two-subband electron system around the LLs crossing points at total filling factor  $\nu=3, 5$ , and 4 where easy-plane or easy-axis QHPF states are well developed. It reveals that the easy-axis quantum Hall pseudo-spin state of  $\nu=4$  is sensitive to the RD-NMR measurement. As approaching to one LL crossing point at  $\nu=4$ , the RD-NMR signal strength and the nuclear-spin-relaxation rate  $1/T_1$  enhance quickly which may be due to the low-energy spin excitations. At another identical LL crossing point of  $\nu=4$ , the RD-NMR signal is found to be suppressed and remains as a puzzle to be understood. Of course further study is necessary to access the detailed mechanism.

This work at USTC was funded by National Basic Research Programme of China (Grants No. 2006CB921900 and No. 2009CB929600), the Innovation funds from Chinese Academy of Sciences, and National Natural Science Foundation of China (Grants No. 10604052, No. 10874163, No. 10804104, and No. 10934006). The work at UCLA was supported by the NSF under Grant No. DMR-0804794.

\*tutao@ustc.edu.cn

†jiangh@physics.ucla.edu

<sup>1</sup>*Perspectives on Quantum Hall Effects*, edited by S. Das Sarma and A. Pinczuk (Wiley, New York, 1997), Chaps. 2 and 5.

<sup>2</sup>V. Piazza, V. Pellegrini, F. Beltram, W. Wegscheider, T. Jungwirth, and A. H. MacDonald, *Nature (London)* **402**, 638 (1999).

<sup>3</sup>E. P. De Poortere, E. Tutuc, S. J. Papadakis, and M. Shayegan, *Science* **290**, 1546 (2000).

<sup>4</sup>K. Muraki, T. Saku, and Y. Hirayama, *Phys. Rev. Lett.* **87**, 196801 (2001).

<sup>5</sup>X. C. Zhang, D. R. Faulhaber, and H. W. Jiang, *Phys. Rev. Lett.* **95**, 216801 (2005).

<sup>6</sup>X. C. Zhang, I. Martin, and H. W. Jiang, *Phys. Rev. B* **74**, 073301 (2006).

<sup>7</sup>K. Lai, W. Pan, D. C. Tsui, S. Lyon, M. Muhlberger, and F. Schaffler, *Phys. Rev. Lett.* **96**, 076805 (2006).

<sup>8</sup>K. Vakili, T. Gokmen, O. Gunawan, Y. P. Shkolnikov, E. P. De Poortere, and M. Shayegan, *Phys. Rev. Lett.* **97**, 116803 (2006).

<sup>9</sup>T. Jungwirth and A. H. MacDonald, *Phys. Rev. B* **63**, 035305 (2000).

<sup>10</sup>D. W. Wang, E. Demler, and S. Das Sarma, *Phys. Rev. B* **68**, 165303 (2003).

<sup>11</sup>X. J. Hao, T. Tu, G. Cao, G.-C. Guo, H.-W. Jiang, and G.-P. Guo, *J. Phys.: Condens. Matter* **21**, 455802 (2009).

<sup>12</sup>G. J. Ferreira, H. J. P. Freire, and J. C. Egues, arXiv:0909.2175 (unpublished).

<sup>13</sup>J. H. Smet, R. A. Deutschmann, F. Ertl, W. Wegscheider, G.

Abstreiter, and K. von Klitzing, *Nature (London)* **415**, 281 (2002).

<sup>14</sup>K. Hashimoto, K. Muraki, T. Saku, and Y. Hirayama, *Phys. Rev. Lett.* **88**, 176601 (2002).

<sup>15</sup>W. Desrat, D. K. Maude, M. Potemski, J. C. Portal, Z. R. Wasilewski, and G. Hill, *Phys. Rev. Lett.* **88**, 256807 (2002).

<sup>16</sup>G. Gervais, H. L. Stormer, D. C. Tsui, P. L. Kuhns, W. G. Moulton, A. P. Reyes, L. N. Pfeiffer, K. W. Baldwin, and K. W. West, *Phys. Rev. Lett.* **94**, 196803 (2005).

<sup>17</sup>I. B. Spielman, L. A. Tracy, J. P. Eisenstein, L. N. Pfeiffer, and K. W. West, *Phys. Rev. Lett.* **94**, 076803 (2005).

<sup>18</sup>N. Kumada, K. Muraki, K. Hashimoto, and Y. Hirayama, *Phys. Rev. Lett.* **94**, 096802 (2005).

<sup>19</sup>N. Kumada, K. Muraki, and Y. Hirayama, *Science* **313**, 329 (2006).

<sup>20</sup>X. C. Zhang, G. D. Scott, and H. W. Jiang, *Phys. Rev. Lett.* **98**, 246802 (2007).

<sup>21</sup>T. Jungwirth and A. H. MacDonald, *Phys. Rev. Lett.* **87**, 216801 (2001).

<sup>22</sup>A. Schmeller, J. P. Eisenstein, L. N. Pfeiffer, and K. W. West, *Phys. Rev. Lett.* **75**, 4290 (1995).

<sup>23</sup>K. Muraki, T. Saku, and Y. Hirayama, *Physica E* **12**, 8 (2002).

<sup>24</sup>K. Hashimoto, K. Muraki, N. Kumada, T. Saku, and Y. Hirayama, *Phys. Rev. Lett.* **94**, 146601 (2005).

<sup>25</sup>Y. Hirayama, K. Murakia, K. Hashimotoa, K. Takashinaa, and T. Sakuc, *Physica E* **20**, 133 (2003).